



**TECHNICAL REPORT
NATICK/TR-01/007**

AD A 388 897

**IN-SITU REAL TIME DETECTION
OF EXPLOSIVE/CHEMICAL COMPOUNDS IN MINES
USING NUCLEAR QUADRUPOLE RESONANCE (NQR)**

by
Andrew D. Hibbs

**Quantum Magnetics
San Diego, CA 92121**

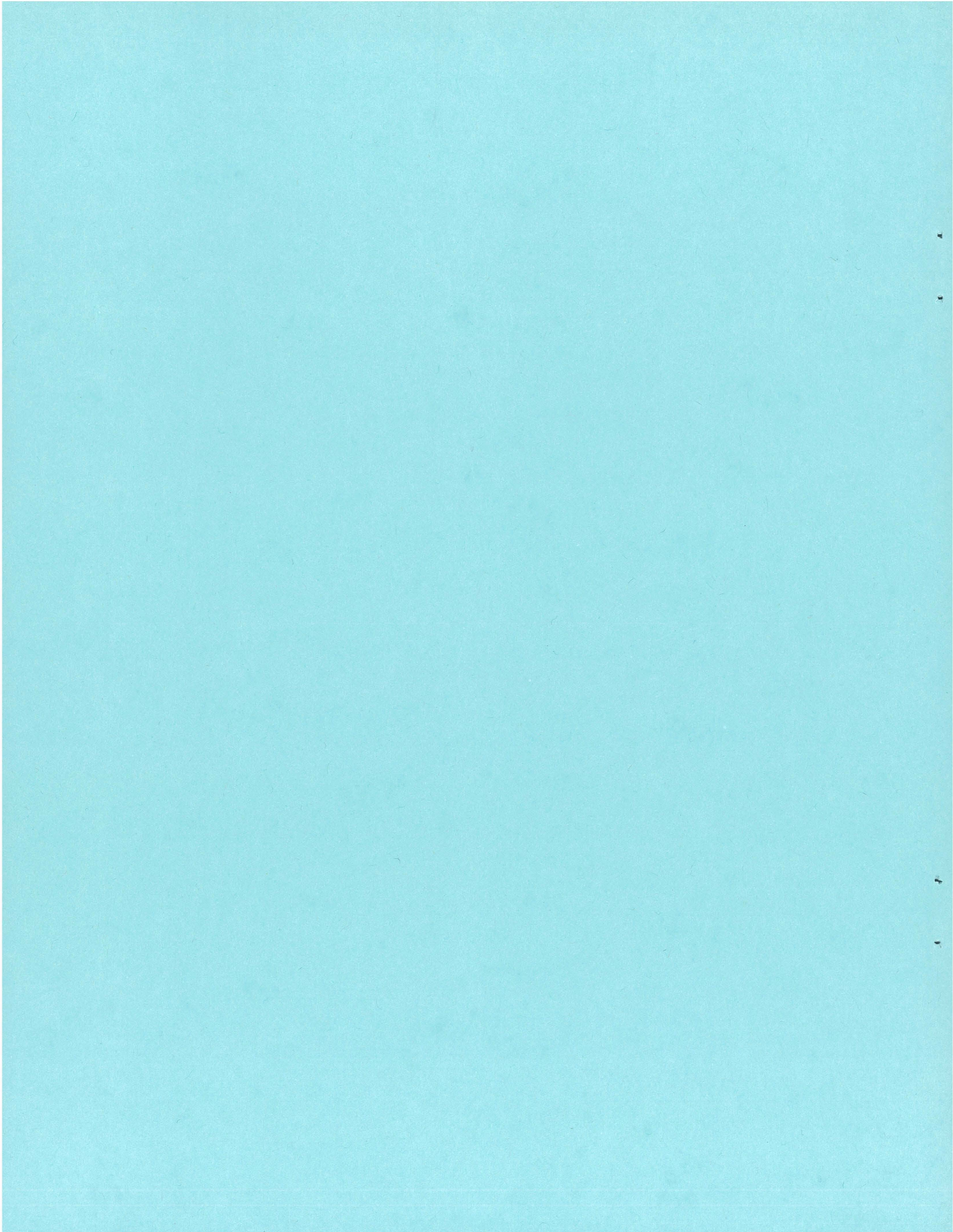
March 2001

Final Report
April 1997 - December 1999

Approved for Public Release; Distribution is Unlimited

**Prepared for
U.S. Army Soldier and Biological Chemical Command
Soldier Systems Center
Natick, Massachusetts 01760-5020**

TECHNICAL LIBRARY
U. S. ARMY NATICK R&D CENTER
NATICK, MA 01760



REPORT DOCUMENTATION PAGE

Form Approved
OMB No. 0704-0188

The public reporting burden for this collection of information is estimated to average 1 hour per response, including the time for reviewing instructions, searching existing data sources, gathering and maintaining the data needed, and completing and reviewing the collection of information. Send comments regarding this burden estimate or any other aspect of this collection of information, including suggestions for reducing the burden, to Department of Defense, Washington Headquarters Services, Directorate for Information Operations and Reports (0704-0188), 1215 Jefferson Davis Highway, Suite 1204, Arlington, VA 22202-4302. Respondents should be aware that notwithstanding any other provision of law, no person shall be subject to any penalty for failing to comply with a collection of information if it does not display a currently valid OMB control number.

PLEASE DO NOT RETURN YOUR FORM TO THE ABOVE ADDRESS.

1. REPORT DATE (DD-MM-YYYY) 30-03-2001		2. REPORT TYPE Final Report		3. DATES COVERED (From - To) April 1997 - December 1999										
4. TITLE AND SUBTITLE IN-SITU REAL TIME DETECTION OF EXPLOSIVE/CHEMICAL COMPOUNDS IN MINES USING NUCLEAR QUADRUPOLE RESONANCE (NQR)				5a. CONTRACT NUMBER C-DAAK60-97-C-9221										
				5b. GRANT NUMBER										
				5c. PROGRAM ELEMENT NUMBER										
				5d. PROJECT NUMBER										
6. AUTHOR(S) Andrew D. Hibbs				5e. TASK NUMBER										
				5f. WORK UNIT NUMBER										
				8. PERFORMING ORGANIZATION REPORT NUMBER										
7. PERFORMING ORGANIZATION NAME(S) AND ADDRESS(ES) Quantum Magnetics 7740 Kenamar Court San Diego, CA 92121				10. SPONSOR/MONITOR'S ACRONYM(S)										
9. SPONSORING/MONITORING AGENCY NAME(S) AND ADDRESS(ES) Sponsor: Defense Advanced Research Projects Agency (DARPA) Advanced Technology Office (Regina Dugan) 3701 North Fairfax Drive Arlington, VA 22203-1714				11. SPONSOR/MONITOR'S REPORT NUMBER(S) NATICK/TR-01/007										
				12. DISTRIBUTION/AVAILABILITY STATEMENT Approved for Public Release; Distribution Unlimited										
13. SUPPLEMENTARY NOTES Monitor: US Army Soldier and Biological Chemical Command, Soldier Systems Center, ATTN: AMSSB-RSS-D(N) (H. Girolamo), Natick, MA 01760-5020														
14. ABSTRACT This program was part of DARPA's "Dog Nose" initiative to develop landmine detection technology based upon the chemical signature of the mine explosive charge. Nuclear quadrupole resonance (NQR) was the only technology pursued that detects the bulk explosive in situ. In the first year the program demonstrated the basic feasibility of using a lightweight coil to measure the explosive RDX (C4) at under conditions typical of antipersonnel and antitank mines. The program also showed for the first time a sufficient TNT signal to make NQR landmine detection feasible. In the second year the program was expanded to improve ruggedness and develop the technology to a more advanced state. A site survey was made to several minefields in Bosnia, and blind tests on TNT and RDX AP and AT mines were carried out at Ft. Leonard Wood. The system detected 100% of all mines in the three tests in the final year, with a false alarm rate less than 1%. Much of the knowledge gained has been only partly implemented in prototypes to date. Further improvements are expected under an Army program to develop an NQR array for route clearance missions, and a Navy program for a man-portable system.														
15. SUBJECT TERMS <table border="0" style="width:100%"> <tr> <td>NUCLEAR QUADRUPOLE RESONANCE</td> <td>LANDMINES</td> <td>CHEMICAL SIGNATURES</td> </tr> <tr> <td>DETECTION TECHNOLOGY</td> <td>MINEFIELDS</td> <td>CHEMICAL COMPOUNDS</td> </tr> <tr> <td>EXPLOSIVE COMPOUNDS</td> <td>MINE DETECTION</td> <td>EXPLOSIVE CHARGES</td> </tr> </table>						NUCLEAR QUADRUPOLE RESONANCE	LANDMINES	CHEMICAL SIGNATURES	DETECTION TECHNOLOGY	MINEFIELDS	CHEMICAL COMPOUNDS	EXPLOSIVE COMPOUNDS	MINE DETECTION	EXPLOSIVE CHARGES
NUCLEAR QUADRUPOLE RESONANCE	LANDMINES	CHEMICAL SIGNATURES												
DETECTION TECHNOLOGY	MINEFIELDS	CHEMICAL COMPOUNDS												
EXPLOSIVE COMPOUNDS	MINE DETECTION	EXPLOSIVE CHARGES												
16. SECURITY CLASSIFICATION OF:			17. LIMITATION OF ABSTRACT SAR	18. NUMBER OF PAGES 39	19a. NAME OF RESPONSIBLE PERSON Henry Girolamo, Program Manager									
a. REPORT U	b. ABSTRACT U	c. THIS PAGE U			19b. TELEPHONE NUMBER (Include area code) 508-233-5071									

TABLE OF CONTENTS

LIST OF FIGURES	v
LIST OF TABLES	vii
PREFACE.....	ix
SUMMARY	1
1. INTRODUCTION.....	2
2. IMPORTANT PARAMETERS OF THE NQR MEASUREMENT.....	4
2.1 Overview of the Basic Measurement.....	4
2.2 Pulse Sequence Design	5
2.3 Data Acquisition	7
2.4 Signal Processing.....	7
2.5 Effect of Temperature.....	9
3. NQR HARDWARE FOR LANDMINE DETECTION.....	11
3.1 Basic System Elements	11
3.2 The NQR Coil.....	12
3.3 Cancellation of Radio Interference	13
3.3.1 LMS-based correlation cancellation (single reference channel).....	13
4. PERFORMANCE OF NQR TECHNOLOGY IN DETECTING LANDMINES.....	15
4.1 Site Visit to Bosnia	15
4.1.1 Measurement of Environmental Properties	16
4.1.2 Test on live Explosives.	17
4.2 Detection Results at Ft. Leonard Wood (Fall 1999).	19
4.2.1 System Set Up and Initial Test.....	19
4.2.2 Antitank Mine Detection Blind Test.....	21
4.2.3 Antipersonnel Mine Detection Test.....	25
4.2.4 Summary of Test Results.....	28
5. CONCLUSIONS AND RECOMMENDATIONS.....	29
REFERENCES.....	30

LIST OF FIGURES

Figure 1. QR Detection of Land Mines Approach	4
Figure 2. PAPS-NPAPS NQR Pulse Sequence Timing Diagram.....	6
Figure 3. The Maximum SNR for Detection of TNT in a Fixed Scan Time as a Function of Temperature.	9
Figure 4. SNR for Detection of TNT at Low Temperature Showing the Crossover Between Single and Double Scans.....	10
Figure 5: Generic QR System Architecture.....	12
Figure 6. The Two Main Generations of NQR Coil Developed under the Program.....	12
Figure 7. Signal Flow Chart for Scalar Correlation Cancellation.....	13
Figure 8. Comparisons of RFI Cancellation Algorithms on a Typical Data Set.....	14
Figure 9. NQR System in Mine Fields near Brcko and Dobol, Bosnia	16
Figure 10. Contour Map of System Output for Blind Detection Test outside the Mine Action Center, Eagle Base, Tuzla, Bosnia	18
Figure 11. Contour Map of System Metal Detection Output.....	18
Figure 12. ROC Curve for RDX Taken on October 25.	19
Figure 13. First NQR Measurement of TNT at Ft. Leonard Wood, October 25, 1999.	20
Figure 14. AT Mine Detection Results.	22
Figure 15. Double Scan ROC Curve for a PMA-1A AT Mines at 5-6 cm Taken on the Morning of October 28.....	23
Figure 16. ROC on a PMA-1A Mine at 6 cm. Ten Scans per Data Point- October 29.	23
Figure 17. ROC Curve on a PMA-1A Mine Taken in San Diego	24
Figure 18. (A) TNT, (B) RDX, and (C) Metal Signal Measured versus Miss Distance to the nearest Mine (figure courtesy Reference 4).	25
Figure 19. Results of Single Passes (a) and Scan/Confirm Scheme (b) on 7 PMA-1A TNT-filled AP Mines	26
Figure 20. Image of Output SNR for AP Mine Test	27
Figure 21. In Field ROC Curve on PMA-1A Mine at 7°C.....	27

LIST OF TABLES

Table 1. Example Parameters for a Working PAPS-NPAS NQR Experiment. Total experimental time is ~2 s.	7
Table 2. Summary of Blind Tests of NQR System on Buried Mines	15
Table 3. Decrease in System Detection Sensitivity Related to Output SNR in the Absence of Soil.	17
Table 4. A Summary of the AT Mines used in the Test. The quantities d and h stand for diameter and height.	21
Table 5. A Summary of the AP Mines Used in the Test. The quantities d, h, l, and w stand for diameter, height, length, and width.....	26
Table 6. Summary of Test Results under Blind Conditions on Prototype NQR Landmine Detection System.....	28

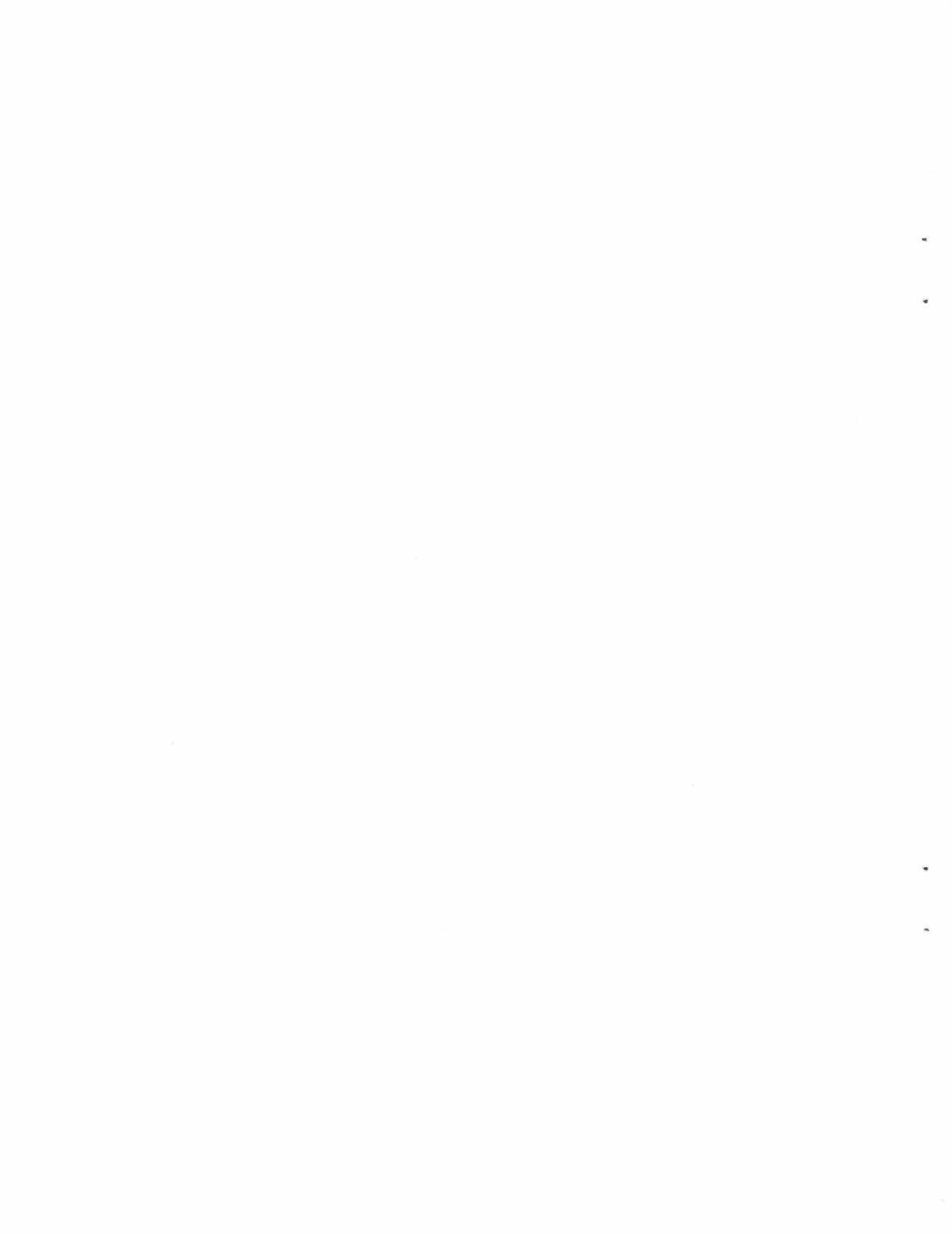
PREFACE

This program was part of the Defense Advanced Research Projects Agency (DARPA) "Dog's Nose" initiative to develop landmine detection techniques based on the chemical signature of the mine. The work was carried out by Quantum Magnetics of San Diego, CA under contract with the US Army Soldier Systems Command, Natick, MA.

This is the final program report covering the period from April 1997 to December 1999. This period comprises the bulk of the DARPA program, in terms of its original goals and scope, and also the work that was added in the second year.

The work relating to development and testing of a vehicle-based nuclear quadrupole resonance (NQR) system that was due to be carried out after December 1999 was rolled into a subsequent follow-on contract funded jointly by the Army and DARPA, and is not part of this report.

Quantum Magnetics wishes to acknowledge and extends its appreciation to Alan Garroway and his research group at the Naval Research Laboratory, for their pioneering achievements in NQR, and their support and assistance during this program. Appreciation is also extended to the following individuals and groups for their support of these efforts: Regina Dugan, DARPA Program Manager; COL Robert Greenwalt, USA (Ret); GY SGT John Crane, USMC, MARCORPSYSCOM; Henry Girolamo, Soldier Systems Command, USA Natick RD&E Center; Vivian George, Walcoff & Associates; the 1st Cavalry and 91st Engineers at Eagle Base, Bosnia; and Camp Pendleton, USMC.



IN-SITU REAL TIME DETECTION OF EXPLOSIVE/CHEMICAL COMPOUNDS IN MINES USING NQR

SUMMARY

This program was part of the Defense Advanced Research Projects Agency (DARPA) "Dog's Nose" initiative to develop landmine detection techniques based on the chemical signature of the mine. NQR was the only effort that focused on detecting the bulk explosive charge of the mine in situ. The other participants in the DARPA program took the route of measuring explosive vapor or particles that had migrated from the mine to the soil surface and thence into the detector.

Significant success was made in the first year, and the program was quickly expanded in scope to build a more rugged system than had originally been proposed, to conduct a field survey in Bosnia, and to take the first steps towards developing a vehicle mounted version of the technology. Success continued in the second year, and at the time of writing, the program has transitioned to the Army for development of a vehicle-mounted NQR coil system and is in the process of transitioning to the Navy for further development towards a fully man-portable system.

Bridging contracts, both augmented by further DARPA funds, were put in place by the Army and Navy in order to maintain program continuity and momentum from the end of the main DARPA program until the new contracts could be set up. This report covers the period from April 1997 to December 1999. This period comprises the bulk of the DARPA program, in terms of its original goals and scope, and also the work that was added in the second year. The work relating to development and testing of a vehicle-based NQR system that was due to be carried out after December 1999 was rolled into the Army bridging contract, and is not part of this report.

This program has been a major technical success, showing for the first time that landmines buried in typical field conditions can be detected by their chemical signature. In the, albeit, limited number of tests at The Army Mine Training School at Ft. Leonard Wood, MO, and in Bosnia, the system has demonstrated detection performance equal to, or better than, any other advanced technology, including those that have been under development for many years. Furthermore, major strides have been made in the understanding of NQR and how to construct NQR systems. Much of this understanding has only partly been incorporated in the prototypes described in this report. The success to date and the new knowledge bodes well for the further improvement of NQR for landmine detection and its eventual contribution to removing the landmine threat.

1. INTRODUCTION

Detection of landmines by the chemical signature of the mine explosive charge is arguably the ideal method to distinguish a mine from its surroundings. In contrast, techniques which are based on the mine shape or metal content will always suffer a false alarm rate that is dominated by the environment clutter.

The most common chemical sensing modality is a canine. Canines, however, did not evolve specifically to address the landmine problem and have a number of well-known deficiencies. Other chemical sensing methods based on vapor detection or particle capture also suffer significantly in field applications owing to humidity, ground contamination and sensor saturation. Furthermore, vapor or particle methods suffer from the explosive transport problem: in order to work at all, some fraction of the mine explosive has to arrive at the sensor.

Nuclear Quadrupole Resonance (NQR) is a chemically specific sensing method that does not require mass transfer from the mine to the sensor. NQR works by interrogating the ground with low frequency radio waves and measuring a unique return signal which only occurs if a mine (or rather its explosive charge) is present. The NQR signal only arises from bulk explosives and is proportional to the explosive mass. This means that fragments of explosive or traces of explosive vapor, both of which are present in post-battlefield conditions, do not cause false alarms. NQR can also distinguish a mine from high levels of metallic clutter and operates through water.

NQR has a short range similar to metal detectors and ground penetrating radar systems. Although in some ways a limitation, the short range allows accurate location of the mine. Overall, the system has the potential to be largely identical in form and usage to a present-day military style metal detector.

Prior to this program, there have been three significant efforts worldwide to develop an NQR-based landmine detection system. Because of the near ideal properties of NQR, these efforts were all quite extensive. None of them succeeded for essentially the same two reasons: a) the large number of basic scientific questions to be answered and b) the overall difficulty of the landmine detection problem. The number of unanswered scientific questions is due to an almost complete absence of research and development in NQR for any other application. This lack of other research has led to an exaggerated assessment of the risks of developing NQR for landmine detection.

In the early 1990s, a major effort was made to apply NQR to the detection of explosives in airline luggage. A number of important breakthroughs were made at the Naval Research Laboratory. These were licensed exclusively to Quantum Magnetics and a number of prototype NQR systems developed and deployed in airports. The NRL breakthroughs related principally to new pulse sequences that reduced the power required and increased the signal-to-noise ratio (SNR) by better isolating the NQR signal. In addition, just prior to submission of the proposal that led to this program, NRL made initial measurements on TNT at room temperature.

There were three principal technical challenges for this program:

1. Development of high sensitivity NQR pulse sequences to detect TNT,
2. Development of an NQR system architecture to detect buried mines, and
3. Development of techniques to remove the background environmental noise.

Underlying these challenges was the need to develop models for the basic physics of the NQR measurement and the interaction of the NQR coil with the ground. In addition, it was necessary to build custom electronic hardware and software for almost the entire prototype system that was developed. In the course of this work, a number of significant engineering improvements were made over previous NQR systems.

Because of the ongoing nature of the development process, and the fact that optimized NQR systems for both vehicle-mounted and backpack applications are already being developed, this report does not contain a detailed description of any of the particular NQR prototypes that were developed. Rather, we provide a general description of the NQR technology and measurement and then discuss in detail the status of the technology in light of the blind tests at Ft. Leonard Wood.

2. IMPORTANT PARAMETERS OF THE NQR MEASUREMENT

2.1 Overview of the Basic Measurement

The system operates by first tuning to the desired resonant frequency of TNT, running the TNT detection sequence, then tuning to the desired resonant frequency of RDX and running the RDX detection sequence. The presence of metal objects is determined from the internal parameters that must be set to tune the system.

QR works by absorption and subsequent re-emission of RF magnetic fields by nitrogen nuclei. For a specific signal to be produced, the nitrogen nuclei must be constrained by the specific electric field environment of the chemical bonds of the explosive compound of interest. This requirement leads to a unique explosive resonant frequency and time dependent QR signature.

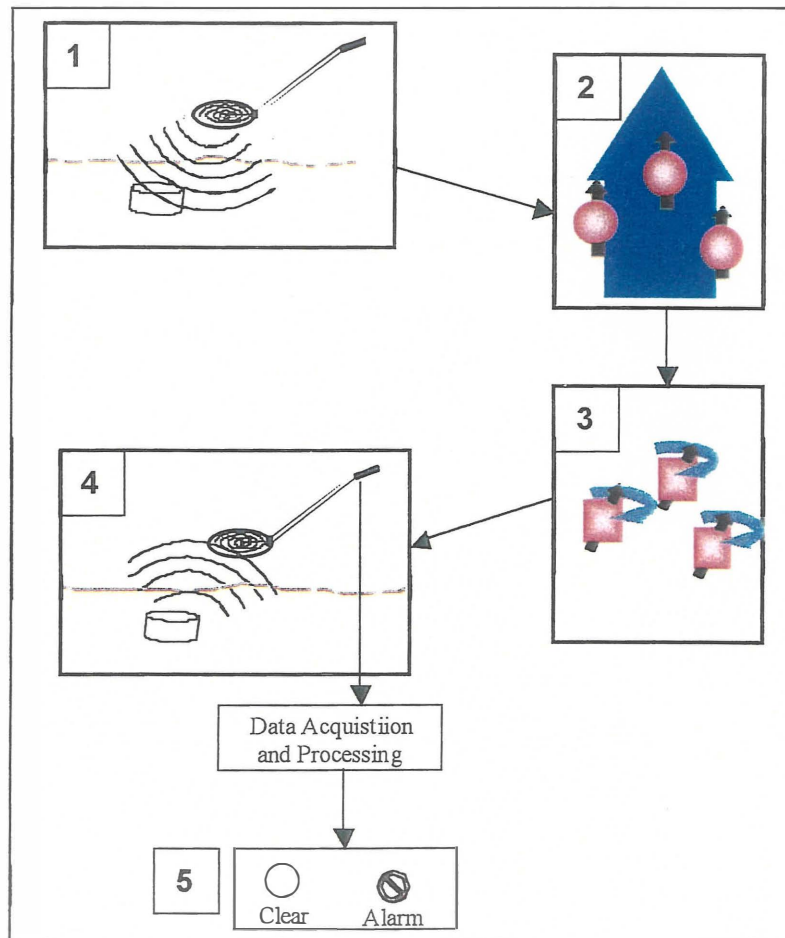


Figure 1. QR Detection of Land Mines Approach

The basic approach to QR detection of land mines is shown in Figure 1. The steps shown in the figure are described below.

1. The detection coil is placed over the region of interest. Roughly speaking, the mine must fall within the projected area of the coil to be detectable (this feature is the same for metal detectors and allows the QR coil to localize the target). The system tunes the QR coil to the frequency of interest: 842 kHz or 741 kHz for TNT, 3.41 MHz for RDX. The system then applies a series of RF pulses of duration ~ 200 microseconds, duty cycle $\sim 30\%$, for about 0.25 seconds.
2. Nuclei magnetic moments within the explosive are momentarily aligned.
3. After each pulse, the nuclei emit a characteristic radio signal, much like an echo, as they return to equilibrium.
4. This signal is picked up by the same coil used to apply the pulse sequence, amplified, and sent to a computer for rapid analysis. At the same time as collecting the signal, the system measures the radio frequency interference (RFI) background of the environment. The environmental signal is subtracted in the system computer.
5. The computer sums the RFI mitigated signal over measurement interval (approximately 0.25 seconds) and compares it against system alarm threshold. The results are presented as either a "Clear" or "Alarm" response for the position(s) scanned.

2.2 Pulse Sequence Design

The nitrogen QR response for RDX and TNT (and most other materials) from a single RF pulse is too small for practical applications; the signal decays in a time of order 10 ms to 50 ms producing a net SNR often below 1. However, precisely timed sequences of RF pulses can extend the time for which the signal can be detected to arbitrarily long lengths in the case of RDX and up to 0.5 seconds in the case of TNT. The net SNR is proportional to the square root of the measurement time and so can be increased to acceptable levels.

Considerable work has been done first at the Naval Research Laboratory and later at QM to optimize the SNR and artifact rejection performance of NQR pulse sequences. A large fraction of the earlier improvement in NQR came from improvements in pulse sequence design. This work is ongoing and will result in separate optimizations for different applications, different environments, and different mine temperatures. However, the basic pulse sequence for RDX gives a good impression of what is involved.

In the field tests to date, a phase alternated pulse sequence – non-phase alternated pulse sequence (PAPS-NPAPS) experiment is used to detect the ^{14}N NQR response of RDX. The particular NQR transition we are currently utilizing lies at around 3.41 MHz. The PAPS-NPAPS sequence is designed to produce the maximum amount of signal per unit time from the RDX ^{14}N nuclei and to vary the phase of the NQR signal in a predictable manner so as to separate it from other artifact signals (e.g. magneto-acoustic ringing and pulse ring-down).

A timing diagram of the PAPS-NPAPS NQR experiment is shown in Figure 2. The Positive PAPS segment of the experiment is repeated n times which corresponds to $2 \cdot n$ separate signal acquisitions. Following the Positive PAPS segments the Positive NPAPS is repeated n times

also. The entire experiment (PAPS and NPAPS) is then repeated with RF pulses of the opposite phase (sign) and with PAPS and NPAPS reversed, which result in NQR signals of the opposite phase (sign) of those produced in the Positive PAPS-NPAPS experiment. We will refer to this second PAPS-NPAPS experiment as Negative PAPS-NPAPS. In the current scheme, Negative PAPS-NPAPS is actually Negative NPAPS followed by Negative PAPS (see Figure 2). Generally, the positive and negative PAPS-NPAPS experiment pair is repeated a number of times (m) in order to improve the sensitivity of the measurement and reject signal artifacts on a shorter time scale.

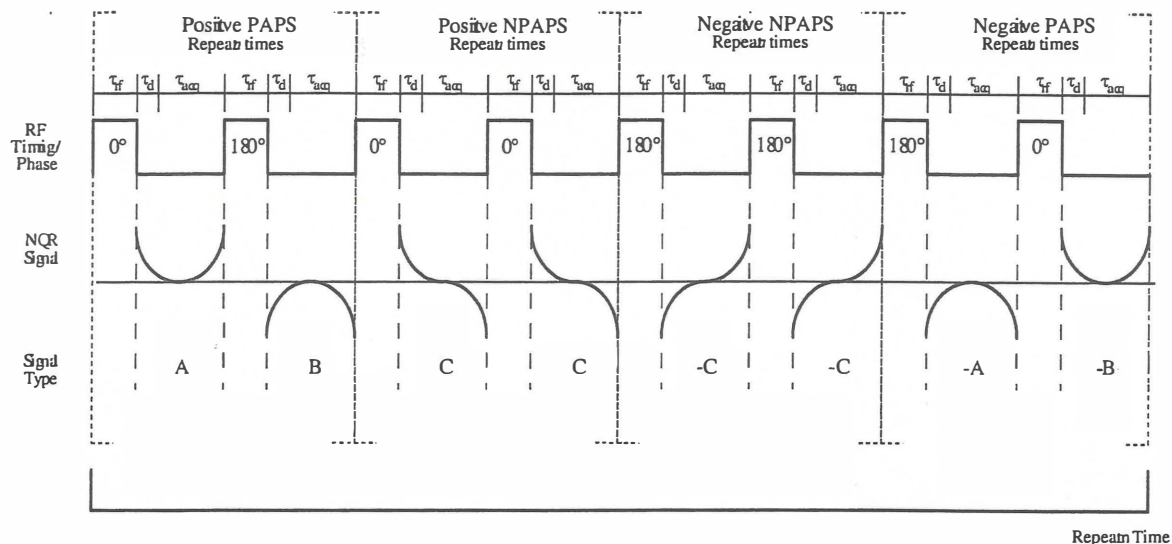


Figure 2. PAPS-NPAPS NQR Pulse Sequence Timing Diagram. Positive PAPS is repeated n times, followed by n repetitions of Positive NPAPS, n repetitions of the Negative NPAPS and n repetitions of Negative PAPS. This entire sequence may be repeated m times to improve sensitivity. The acquired NQR signal comes in six forms - $\pm A$, $\pm B$ and $\pm C$.

The NQR signal in a single segment can be described as the sum of an exponentially decaying signal (FID) with time origin in the middle of the preceding pulse and an exponentially increasing function (ECHO) with time origin in the middle of the following pulse. At the present time, detection is based on the ECHO signal, since this signal can be separated from artifacts which follow the phase of the transmitted RF. Such artifacts include pulse ringdown, piezo-electric ringing and magneto-acoustic ringing. The accumulation procedure used to remove these artifacts also removes the FID component of the signal. It is possible to separately extract the FID component of the signal, but ringing artifacts will likely corrupt the data.

The ECHO signal is actually not present in the very first segment; the ECHO must build up as the NQR spin system reaches a steady state with the excitation pulses. At 25°C , the time constant to reach the steady state is approximately 10 ms. When the sequence changes from PAPS to NPAPS, the ECHO signal must build up again. Therefore, it is necessary to have n large enough so that the ECHO signal is present during a significant portion of PAPS and NPAPS. In order to keep the time scale of the artifact rejection short, n must not be made too large. The current system configuration has ~ 125 ms PAPS and NPAPS sequences.

2.3 Data Acquisition

In each case n_{acq} complex data points or samples are acquired during each acquisition period (τ_{acq}); each set of n_{acq} complex data points is referred to as either an acquisition segment or simply a segment. The acquired signal is comprised of complex data points which represent the two-phase components of the NQR magnetization (0° and 90° with respect to the RF carrier). The NQR signal is demodulated with respect to the RF transmitter frequency and then digitized at a rate of ν_{acq} ; ν_{acq} is limited by the current spectrometer software to be no greater than ~ 700 kHz. A variety of experimental conditions affect the precise NQR frequency, so in general the demodulated signal will be slightly off resonance with respect to the excitation frequency. The deviation from zero frequency, $\delta\nu$, is not expected to exceed ± 5 kHz.

Pulse-pulse ringdown saturates the pre-amplification circuitry and prevents signal acquisition immediately following the RF pulse. Therefore, signal is not acquired until some time, τ_d , after the RF pulse. The required duration of τ_d depends upon both the system hardware and the ability of the signal-processing algorithm to differentiate the NQR signal from the pulse-pulse ringdown. In Table 1 we list the experimental parameters which provide the maximum detection sensitivity per unit time for a specific NQR system at QM. Under these conditions, if $\nu_{acq} = 200$ kHz, then 80 complex data points are acquired per segment. Due to the nature of the NQR interaction, if certain of the parameters are changed, the peak NQR SIGNAL will be reduced. In particular, increasing τ_{acq} , decreasing n , or decreasing τ_{rf} will reduce the NQR signal intensity. Decreasing τ_d increases the amount of interfering signal from ringing artifacts, but it does not necessarily reduce the absolute NQR signal intensity.

Table 1. Example Parameters for a Working PAPS-NPAS NQR Experiment.
Total experimental time is ~ 2 s.

Parameter	τ_{rf}	τ_d	τ_{acq}	n	n_{ave}	n_{acq}	ν_{acq}
Value	170 μ s	60 μ s	530 μ s	326	1	106	200 kHz

2.4 Signal Processing

Currently, the data collected from a complete PAPS-NPAS experiment is processed in the following manner. First, all of the separate acquisition segments ($\pm A$, $\pm B$, $\pm C$) are accumulated into a single segment containing a total of n_{acq} complex data points. The accumulation is a simple vector adding of all of the segments following a multiplication by ± 1 . The rules for the sign multiplication are as follows:

$$+1 \cdot A, -1 \cdot (-A), -1 \cdot B, +1 \cdot (-B), -1 \cdot C, +1 \cdot (-C). \quad 1$$

The data resulting from the accumulation operation is a monotonically increasing function since the FID signals of the -C segments cancel out the echo signals of the A and -B segments. Furthermore, the first few (one or two) segments acquired differ substantially from later

segments since the spin system has not reached a steady state until a number of RF pulses have been applied. The ECHO component of the NQR signal is identically zero in the first segment and exponentially increases to a constant value in succeeding segments. Ignoring the irregularities of the first few segments, the accumulated dataset is generally assumed to be a single exponential but may be a multi-component exponential or a Gaussian. If we assume the data to be a single, increasing exponential, then the form of the remaining signal is given by

$$S(t) = S_0 e^{-(\tau_{acq}-t)/T_2^*} \cdot e^{i(\delta\nu t + \phi)}, \quad 2$$

where t defines the time evolution from the end of one pulse to the beginning of the next, $\delta\nu$ is the frequency offset, and ϕ is the phase of the signal. The time constant T_2^* is assumed to not vary considerably between samples, but large temperature gradients in the sample can significantly shorten T_2^* . We generally assume that $T_2^* = 800\mu s$ for the 3.41 MHz NQR transition of RDX. The signal phase, ϕ , does not vary considerably and is generally considered to be a fixed parameter.

In order to simplify the explanation of the current signal processing we will reverse the sense of the time evolution so that we have an exponential decay with a maximum at zero time; this corresponds to merely flipping the signal dataset end for end. The signal now has the form

$$S(\tau) = S_0 e^{-\tau/T_2^*} \cdot e^{-i(\delta\nu\tau + \phi)}, \quad 3$$

where $\tau \equiv \tau_{acq} - t$.

The Fourier analysis of the signal begins with the application of an exponentially decaying matched filter given by

$$G(\tau) = e^{-\tau/T_2^*}, \quad 4$$

followed by zero-filling which results in a dataset with approximately $4n_{acq}$ to $8n_{acq}$ data points. The zero filling is performed to provide interpolation between points in the frequency domain and has been shown experimentally to improve the performance of the overall signal processing strategy. The apodized and zero-filled data is then Fourier transformed to yield the NQR frequency spectrum. In one implementation, the final operation consists of measuring the maximum amplitude of the magnitude of the spectrum within the frequency range of interest (e.g. ± 2 kHz). In the other implementation the spectrum is phase “corrected” and the maximum amplitude of the real component of the spectrum is measured; the phase correction compensates for a non-zero value of ϕ' and the fact that the first point of $S(\tau)$ is actually shifted away from the true zero-time point. For both approaches, the peak amplitude, A_0 , indicates the presence of RDX if greater than or equal to A_{tol} and the absence of RDX if less than A_{tol} . Due to the presence of noise and signal artifacts, the determination of A_{tol} is always a trade off between sensitivity and false alarm rates.

2.5 Effect of Temperature

For TNT, the explosive temperature is one of the most important variables in determining the total NQR signal that can be acquired under practical conditions. The temperature dependence for RDX is much less than for TNT and can be accommodated into any scheme adopted to address the temperature effects for TNT.

The overall effect on the TNT SNR at a function of the total measurement time is shown in Figure 3. The black line shows the SNR for a double scan if the sample is allowed to fully relax between measurements. At around 25°C the sample is essentially fully relaxed in 10 seconds. Further increases in SNR at 25°C can be achieved by making additional scans if time allows; e.g. scanning for 60 s would be approximately 6 scans. Before the Ft. Leonard Wood tests a complete matrix of the optimum number of scans for a given repeat time was drawn for the expected range of mine temperatures.

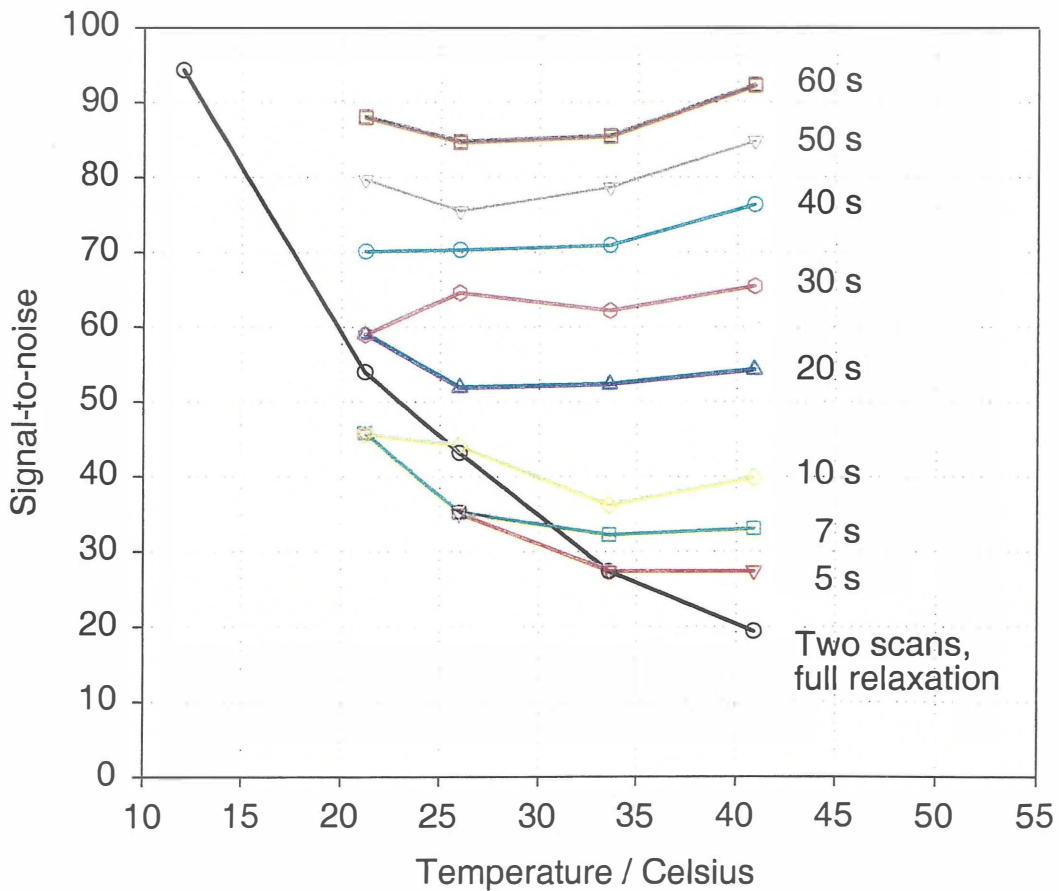


Figure 3. The Maximum SNR for Detection of TNT in a Fixed Scan Time as a Function of Temperature.

The effect on the TNT SNR at lower temperature is shown in Figure 4. The blue line is the SNR for two scans fully relaxed and is the same as the black line in Figure 3. Figure 3 and Figure 4 illustrate the competing temperature dependent processes in TNT. Both the signal coherence time (T_2^*) and the thermal relaxation time (T_1) decrease with increasing temperature. The result

is that at low temperature the SNR from a single pulse sequence is relatively high, but only a single sequence can be run in a reasonable period of time (e.g. 30 seconds). At high temperatures, the single sequence SNR is low (see red line in Figure 4), but the sequence can be rerun several times. For a given time period the single and multisequence regimes meet at a shallow minimum of the SNR vs. time response. For example, for a 30 second scan time, the crossover occurs around 17°C.

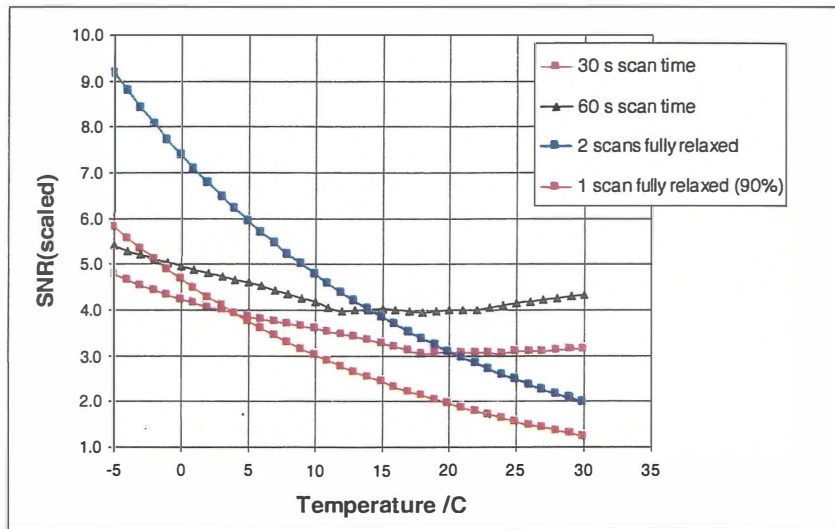


Figure 4. SNR for Detection of TNT at Low Temperature Showing the Crossover Between Single and Double Scans.

Above the crossover point the T_1 and T_2^* temperature dependences largely cancel as far as the signal-to-noise ratio is concerned. For temperatures above 20°C, TNT can be detected with essentially constant sensitivity if rescanning is employed.

3. NQR HARDWARE FOR LANDMINE DETECTION

3.1 Basic System Elements

The generic QR system architecture for a single coil system is shown in Figure 5. It is broken down into the following elements:

- 1) Detection Coil Element
 - a) This coil is used for pulse transmit and QR signal pick-up. The actual coil is made of one or more turns of copper. The detection coil element includes the following electronics, much of which is lumped into a sub-element called the Probe Electronics Package (PEP):
 - i) Tuning capacitors and relays
 - ii) Coupling circuit between the transmit amplifier and the coil
 - iii) Tuning relay control
 - iv) Front-end receiver electronics
 - (1) Low noise preamplifier (amplifies the QR response signal)
 - (2) Q-Damper (to quickly take the energy out of the coil after a transmitted pulse)
 - (3) Preamplifier protection circuitry
- 2) Transmit Amplifier
- 3) RFI Cancellation Antennas and associated electronics
- 4) Data Acquisition and Computer
 - a) Computer that controls the system, processes the data, and hosts the operator interface
 - b) Data Acquisition module
 - i) Generates RF pulses
 - ii) Digitizes and filters RF from QR detection coil(s) and RFI antennas
 - iii) Control interfaces to the detection coil and RFI electronics
 - iv) Limited signal processing (if a processor is on the module – otherwise, signal processing is done on the computer)
- 5) Power Supplies

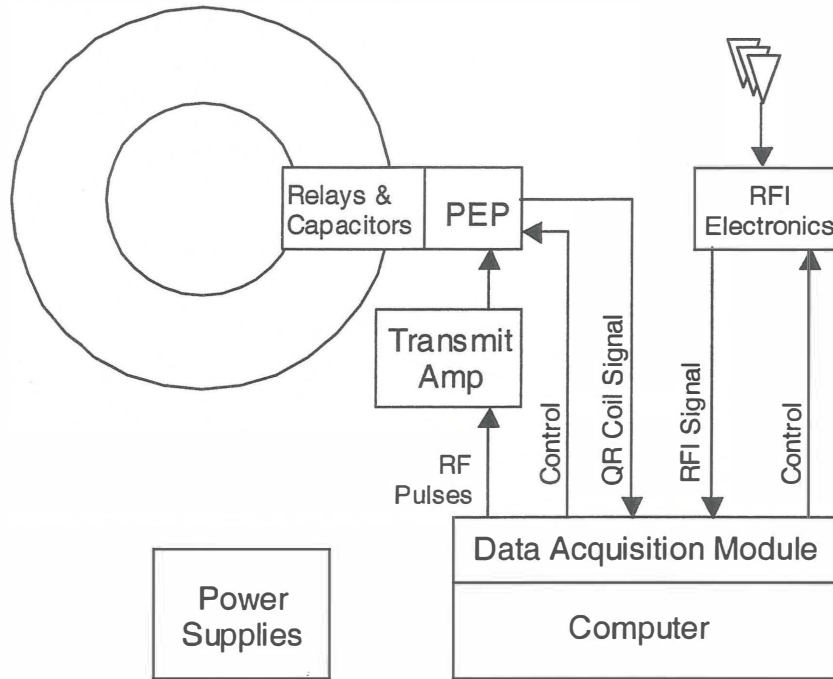


Figure 5: Generic QR System Architecture.

3.2 *The NQR Coil*

The NQR detection coil has gone through a number of configurations as the technology has improved and data has been collected in the field. The two main generations of coil design are shown in Figure 6. On the left is the gradiometer coil design developed in the first year of the program. In this design, the coil close to the ground measures the NQR signal plus background environmental radio noise, while the upper coil measures only the background noise. The coils are wound in a different sense and connected in series so that in principal the background field is cancelled out. In practice, the background RF field was found to vary too strongly in the immediate vicinity of the ground for sufficient cancellation to occur.

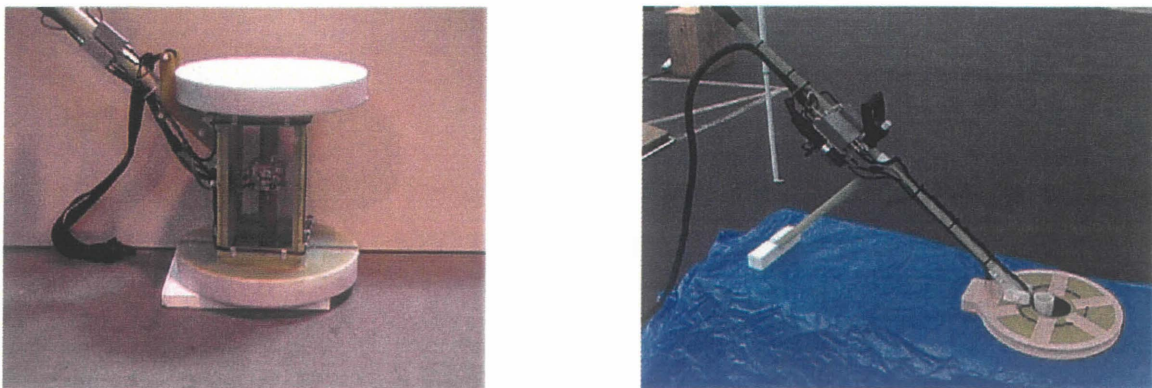


Figure 6. The Two Main Generations of NQR Coil Developed under the Program.

The right hand image of Figure 6 is the single coil approach used for the Bosnia and later Ft. Leonard Wood tests. In this case, the background environmental radio noise is measured on a completely separate set of antennas and subtracted in the main computer using an adaptive algorithm (see Section 3.3). The single coil configuration is lighter and has a higher sensitivity than the gradiometer coil.

3.3 Cancellation of Radio Interference

3.3.1 LMS-based correlation cancellation (single reference channel)

The present NQR mine detection system uses a standalone reference antenna or pair of antennas to measure the local radio frequency interference (RFI). The RFI information is then subtracted from the signal channel using a least mean square (LMS) algorithm, as shown schematically in Figure 7.

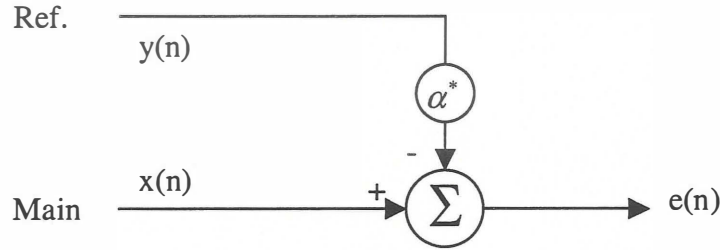


Figure 7. Signal Flow Chart for Scalar Correlation Cancellation.

The reference signal is adaptively scaled and subtracted from the main channel (the detection coil signal), using a frequency-domain implementation of LMS-based correlation cancellation. The incoming data is converted into the frequency domain using a discrete Fourier transform (DFT). Each DFT coefficient represents the sampled output of a digital narrowband filter at a specified frequency. The sequence of DFT coefficients computed over time at a single DFT bin is considered as a time series. For each DFT bin, two such “time series” are produced: one for the main channel, and one for the reference channel.

The subtraction weights, α , are calculated via the LMS recursion:

$$\begin{aligned}
 e(n) &= x(n) - \alpha^*(n)y(n) \\
 \alpha(n+1) &= \alpha(n) + \mu(n)e^*(n)y(n) \\
 \mu(n) &= \frac{\mu_{LMS} \cdot 2}{P_y}
 \end{aligned}
 \tag{Equation 5}$$

where P_y is the average reference channel power. For convergence, $0 < \mu_{LMS} < 1$. Typically we use $\mu_{LMS} = 0.05$. In practice, it is necessary to estimate the reference channel power recursively. We currently use the recursion:

$$P_y(n+1) = (1 - \lambda)P_y(n) + \lambda(|y(n)|^2)
 \tag{Equation 6}$$

$$0 < \lambda < 1$$

Equations 5 and 6 can be easily extended to multiple reference antennas and to the case in which the coefficients are calculated based on a number of data points in the time series data stream (taps) instead of just one. Using this algorithm, significant cancellation of RFI could be achieved depending on the site and time of day. A typical result for Camp Pendleton is shown in Figure 8. It was found that, in general, there was no improvement in going from 1 to 3 taps for the algorithm, and in later tests, only 1 tap was used.

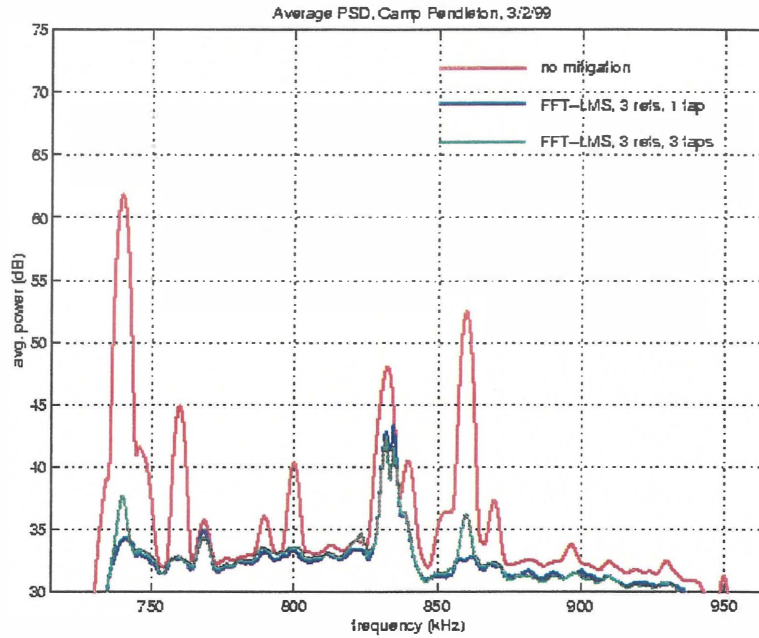


Figure 8. Comparisons of RFI Cancellation Algorithms on a Typical Data Set.

4. PERFORMANCE OF NQR TECHNOLOGY IN DETECTING LANDMINES

Outdoor blind detection tests using live explosives were carried out at regular intervals throughout the program. The test date and purpose for all such tests are summarized in Table 2.

Table 2. Summary of Blind Tests of NQR System on Buried Mines

Date	Type	Location	Notes
May 98	RDX milestone tub test	QM facility	> 14,000 measurements
Sept 98	RDX outdoor lane tests	DARPA Test Site (Ft. LW)	100 m lane
Mar 99	RDX grid	Camp Pendleton CA	New coil design
July 99	Ground survey and RDX	Bosnia (various) and MAC*	Repeated move and set up
Aug 99	TNT tub demonstration	QM facility	Significant RFI
Oct 99	Buried TNT/RDX AT mines	DARPA Test Site (Ft. LW)	System fault ended test
Dec 99	Buried TNT/RDX AP mines	DARPA Test Site (Ft. LW)	Continue October test

* Mine Action Center, Eagle Base Bosnia

Results of these tests have been published in references [1], [2], and [3]. In addition, an extensive tests report on the TNT & RDX detection tests at Ft. Leonard Wood in October & December 1999 has been prepared by the outside evaluation team [4]. In this report, we elaborate in more detail on the site visit to Bosnia and on the overall system performance at the most recent Ft. Leonard Wood tests.

4.1 Site Visit to Bosnia

In November 1998, the DARPA program manager visited various minefields in Bosnia to observe at first hand the mine clearance operation. Contacts were made with the in-theatre engineers and demining teams, and an invitation was extended to operate systems developed under the DARPA program along side deminers in Bosnia. Accordingly, it decided to bring out an RDX-only NQR system at the first opportunity in order to gain sufficient experience to take part in a true mine clearance test involving RDX and TNT mines as soon as the technology would allow.

There were three specific goals for the site visit. Firstly, we wished to determine whether the soil conditions in known Bosnian minefields would be detrimental to an NQR measurement. In particular, a possibility was raised that laterite soil known to be present in some minefields in Bosnia might affect a magnetic-based system. In addition, from experience gained in airline security, we were concerned that debris in the vicinity of minefields might cause significant interference. Secondly, we were concerned about whether any radio transmitters with emissions at 842 kHz were operated within range of possible sites, and if so, whether the fields were sufficiently uniform to be cancelled by the RFI mitigation system. Thirdly, we wished to find out from direct experience the practical challenges that a final system would encounter.

The intermediate prototype system (detecting RDX and metal-cased mines only) was tested at camp Pendleton in June and shipped approximately one month before the test. The system was unpacked in a side hangar at Eagle Base and then moved to a disused MIG bunker on a side road. The system was left on the back of a standard military five-ton truck for the whole time in the field. During later tests, it was found that the system actually bounced clear of the truck bed at even slow driving speeds and significant damage to the metal structure resulting in shearing a number of welds occurred before the end of the visit.

4.1.1 Measurement of Environmental Properties

The system was operated at a total of 5 locations in Bosnia in July 1999. Three of these were areas within actual minefields that were in the process of being demined, although the areas were deemed to be clear of mines. The soil properties were assessed via their resistive loading effect on the NQR detection coil and by the level of piezo-electric and magneto-acoustic ringing produced by the NQR RF excitation pulse. The former is easily determined by the measurement of the coil quality factor, Q , that is automatically done prior to each QR measurement. If present, the soil ringing properties are evident in the time interval immediately after the RF pulse.

Weather conditions were typical for the time of year and steady light rain was encountered at the three minefield sites and on the day of the test at the Mine Action Center. Typical scenes are shown in Figure 9. Between 40 and 100 double measurements of the Q and ringing were made at each minefield. No ringing was observed at any of the sites measured.



Figure 9. NQR System in Mine Fields near Brcko and Dobol, Bosnia. The electronics rack is on the back of the truck.

The loading effect of the soil conductivity leads to a decrease in the system sensitivity. The average decrease in system detection sensitivity, as quantified by the output signal-to-noise ratio (SNR), at all the sites visited in Bosnia is summarized in Table 3.

Table 3. Decrease in System Detection Sensitivity Related to Output SNR in the Absence of Soil.

Site	Reduction in RDX Sensitivity due to Soil Conditions	Notes
Eagle Base Checkpoint #44	15%	Dry conditions, road side vegetation
Mine Field #2620 (Dobol)	27%	The reduction in TNT sensitivity would be <4%
Mine Field #1024 (McGovern), site 1	22%	Considerable building debris
Mine Field #1024 (McGovern), site 2	12%	The reduction in TNT sensitivity would be <2%
Eagle Base Mine Action Center	31%	Site of RDX blind detection test

The environmental radio frequency noise was much lower than sites in the US. A small signal at 830 kHz was observed from the direction of Belgrade, and one at 740 kHz from the direction of Brcko. Comparable signals were found in all three reference channels, which leads us to believe that these signals could be well cancelled by our RFI mitigation algorithms.

4.1.2 Test on live Explosives.

A blind test of RDX detection performance was conducted in a picnic area immediately outside the Mine Action Center at Eagle Base. This area was highly cluttered with debris, which was partly cleared during system set up, and was located very close to several small parking areas. The communications center for Eagle Base was located adjacent to the picnic area, and a large bulldozer was operating within 100 m of the site. There had been intermittent light rain for the previous two days and the ground was very wet.

The DARPA representatives buried five 50 g pieces of RDX and two 570 g RDX sticks in a 3 m x 3 m test area, to simulate five small antipersonnel (AP) mines and two antitank (AT) mines respectively. One PROM 1 metal cased mine and nine 5.56 mm spent cartridges were also buried. A smoothed contour plot of the raw system output of the RDX and metal detection data is shown in Figure 10.

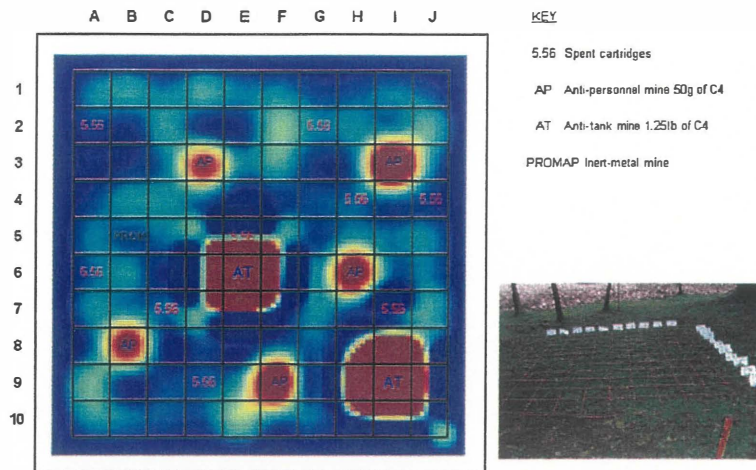


Figure 10. Contour Map of System Output for Blind Detection Test outside the Mine Action Center, Eagle Base, Tuzla, Bosnia. Target type is superimposed, PD = 100%, PFA = 0%.

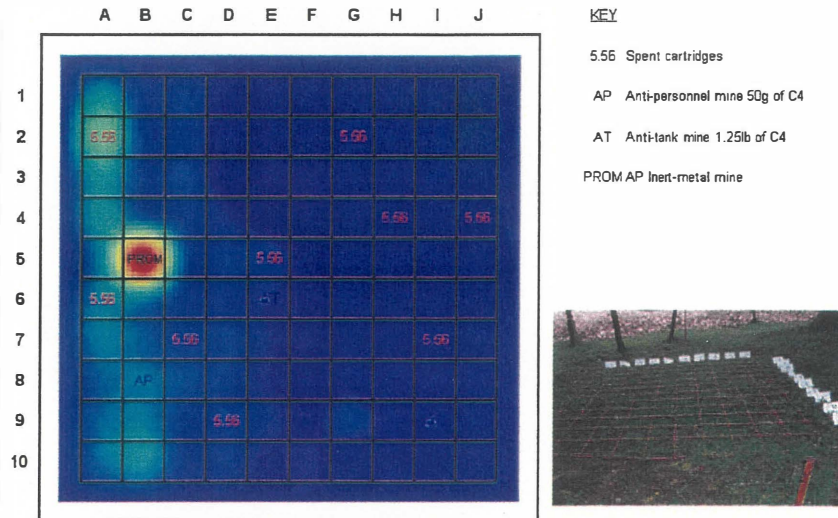


Figure 11. Contour Map of System Metal Detection Output. Data obtained simultaneously with results of Figure 10.

The system was operated during the test by a Marine Corps Gunnery Sergeant, without assistance from the system developers. The user was able to correctly locate all eight mines during the test with zero false alarms. Immediately prior to the test, the same operator using a military metal detector located two of the mines with 34 false alarms. The RDX measurement time was 2 seconds per cell. Initial detections were rescanned twice and a 2 out of 3 voting procedure employed.

4.2 Detection Results at Ft. Leonard Wood (Fall 1999)

4.2.1 System Set Up and Initial Test

The complete NQR prototype system, capable of detecting TNT as well as RDX and metal cased mines, was first taken to the DARPA test site at Ft. Leonard Wood in late October 1999. The system was driven from San Diego and arrived mid-morning on Sunday, October 24. The system was driven directly to the test site and unpacked.

This was the first time that the complete multicomponent system with its new rack of electronics had been shipped, and so the system was carefully checked before operating at full power. An initial ROC curve on a VS50 RDX mine was taken at about 8:30 p.m. on Sunday evening. The performance was disappointing at the level of 90% PD at 20% PFA. The RDX sample was remeasured the following Monday. The standoff was 5 cm, the mine temperature was in the range 5 – 10 °C, and the scan time was set to 3 seconds. The resulting ROC is shown in Figure 12.

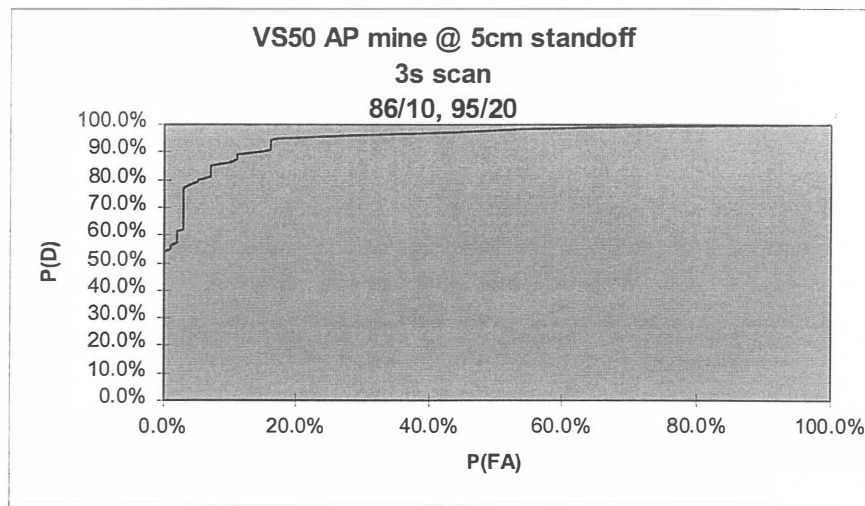


Figure 12. ROC Curve for RDX Taken on October 25.

Compared to previous results on RDX, this result was clearly disappointing. In previous tests in QM's parking lot and even in Bosnia, we would expect to achieve close to 100% PD at 0% PFA under these conditions. The poor performance on RDX was attributed to three possible causes:

- RDX detection was not optimized prior to the test. In fact, owing to focus on TNT, no accurate RDX data was taken with the system prior to this test.
- The mine temperature may have affected the measurement. Efforts focused on the effect of temperature on TNT detection but only minimally on RDX.
- There may have been interference, either self-induced via system damage or from a remote source, that degraded the measurement. Several problems of this kind were found during the first RDX test at Ft. Leonard Wood in September 1998.

There was insufficient time to resolve these questions in the field, and given that RDX detection capability had been established earlier, attention was immediately switched to detecting TNT.

The first ever in-field ROC curve on TNT is shown in Figure 13. The data was taken around lunchtime, and the mine temperature was estimated to be 15°C.

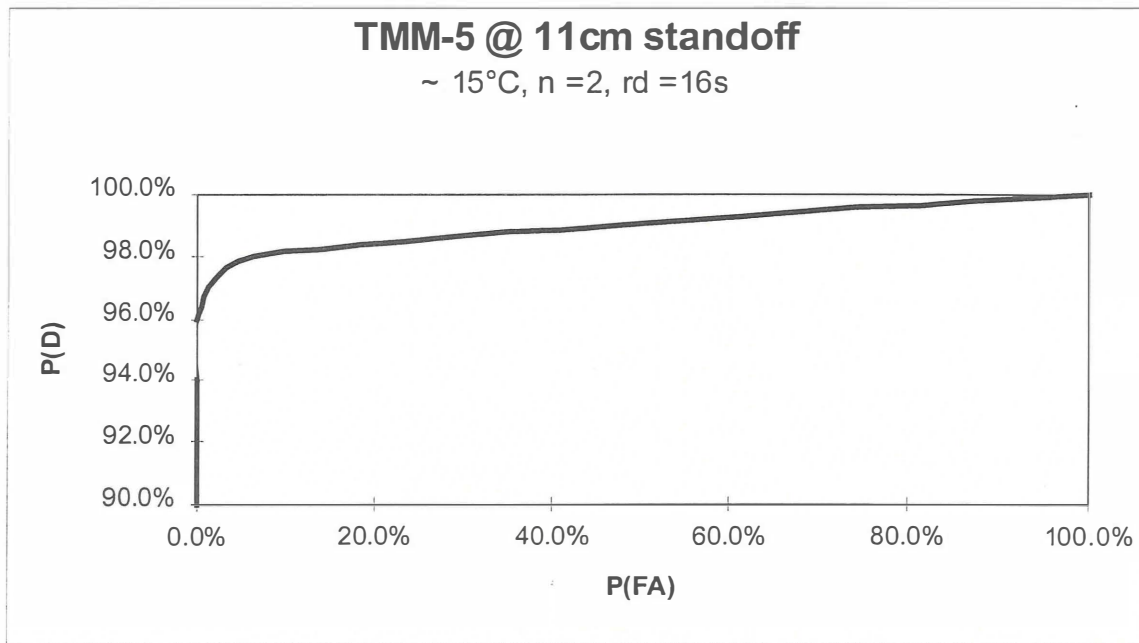


Figure 13. First NQR Measurement of TNT at Ft. Leonard Wood, October 25, 1999. The Center of the mine explosive charge was at 18 cm.

This ROC curve was actually better than expected by a factor at least 50% (in SNR). The SNR determined from Figure 13 was 5.0. A second set of background noise data was taken and another ROC curve plotted using the same TNT data with the new noise data. The result for this was actually better than shown in Figure 13, achieving 98% PD at 0 PFA. It is human nature not to worry unduly when things turn out better than expected, and no specific action was taken to investigate the reason for the better than expected result. However, it is instructive, and provides an important perspective, to consider the possible causes of the discrepancy in our projections.

- a. Inaccurate scaling for large standoff. Prior to October 24, QM had not had access to a TNT AT mine (owing to the large amount of explosive involved). Because of the thermal relaxation time of TNT, it is very time consuming to measure very small TNT signals. As a result, all previous standoff TNT NQR measurement were on AP mines at 6 cm or nearer.
- b. Quality of TNT Sample. In all projections, QM assumed that the NQR signal per unit mass for TNT would be that of the PMA-1A AP mine. This mine was chosen for scaling because it has the smallest signal per unit explosive mass of any of the samples measured by QM. It is quite possible, even likely, that the signal per unit mass of the TMM-5 was larger than that of the PMA-1A.
- c. Inaccurate calibration for temperature. The mines available for initial test at the DARPA test site were stored overnight in a shallow hole partly covered with a plastic sheet and loose earth. At 7:00 a.m. on October 25, these mines had frost on them. Later in the day,

at the time of the test, the explosive surface temperature was around 15°C based on a surface measurement using a handheld probe.

Based on the RDX and TNT measurements, we decided to proceed with the AT mine blind test. The detection thresholds were set based on the background noise data sets used for Figure 12 and Figure 13.

4.2.2 Antitank Mine Detection Blind Test

The inner and outer diameters of the coil for the new two-compound detection head were optimized for detection of AP mines. For AT mines, the coil actually samples only about half of the total volume of explosive present and so is relatively inefficient. Nevertheless, it was considered valuable to investigate the detection performance on buried AT mines, to project the performance of a possible vehicle-based NQR detection system.

To simulate the operation of the vehicle mounted QR system, the TNT detection time was set to 0.25 seconds. This is approximately the amount of time a mine would be under a 60 cm diameter QR detection coil moving at 7 kph. The mine lane was 26 m in length by 1.12 m wide. There were 20 TMA-4, 2 Type 72, and 1 TMM-1 AT landmines buried at 2 cm to 5 cm overburden. The mine characteristics are summarized in Table 4.

Table 4. A Summary of the AT Mines used in the Test. The quantities d and h stand for diameter and height.

AT Model	Case Material	Main Charge	Size (CM)	Country of Origin
TMA-4	Plastic	5.5 kg TNT	d=28.4, h=11	former Yugoslavia
Type 72	Plastic	5.4 kg TNT/ RDX (50/50)	d=27, h=10	China
TMM-1	metal	5.6 kg TNT	d=30, h=9	former Yugoslavia

This test was actually the first time we had tried to operate a QR system in scanning mode when detecting TNT. Owing to miscellaneous delays associated with logging the data and moving the trailer, the lane was scanned in two halves on separate days. The results for each half are shown in Figure 14. Also shown in Figure 14 is the mine position as determined by a prior GPS measurement.

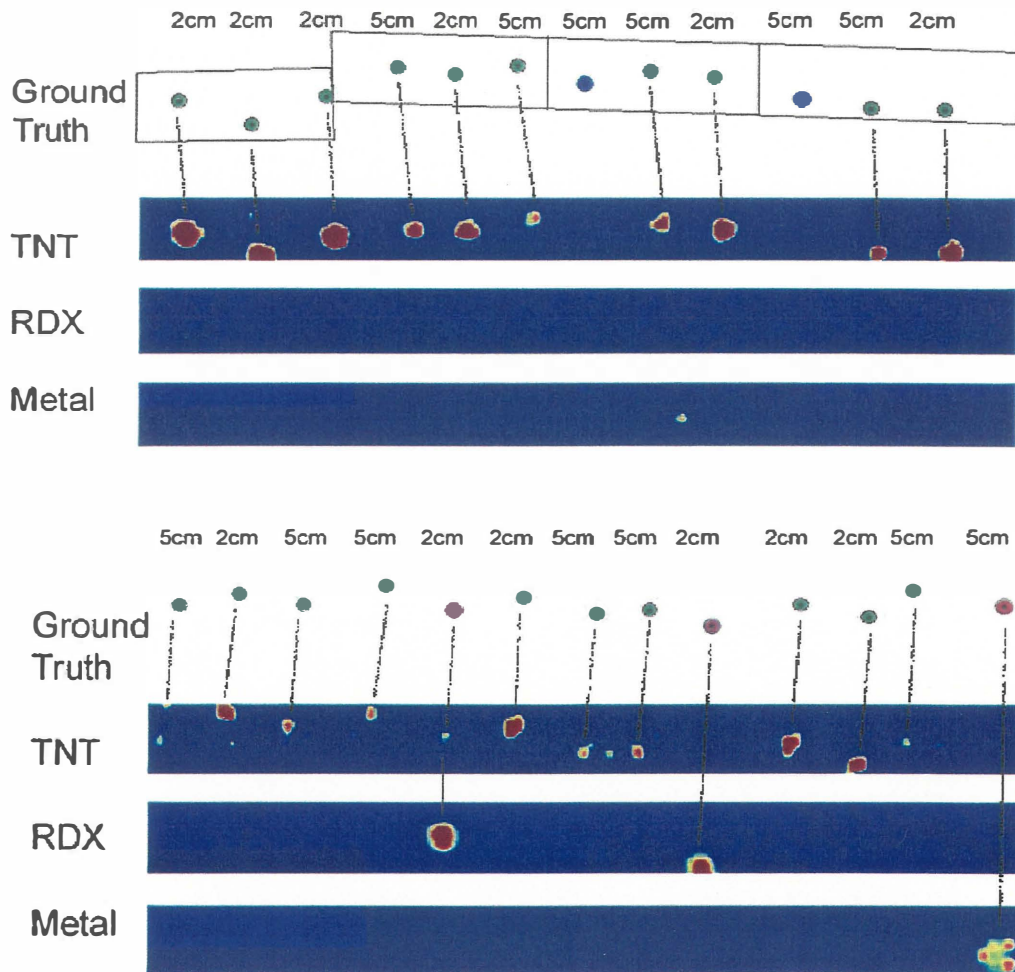


Figure 14. AT Mine Detection Results. Upper data, eastern half of lane, measured on October 26. Lower data, western half measured on October 28.

There were no RDX or TNT mines present in the eastern half of the lane. However, the smaller peaks in the TNT data for the western half suggest that the system performed less well on October 28. This apparent lack of performance can be corroborate by other measurements done around this time.

On October 27, the system was tested on AP mines. However, the test was abandoned when it appeared that the system was producing non-reproducible results. On the morning of October 28 (i.e. before the test on the western half of the AT mine lane), an ROC was taken on a PMA-1A mine at 5 to 6 cm standoff. The result, shown in Figure 15, is dramatically worse than was expected. The result was, in fact, considerably worse than obtained in a blind test in the QM parking lot in August, where a high level of RFI was present. From these independent measurements, it is clear that significant system degradation occurred between October 26 and October 28.

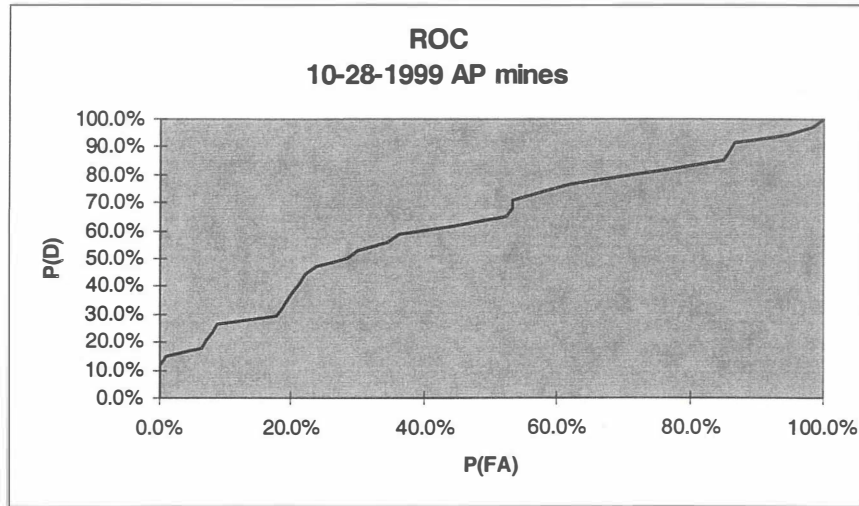


Figure 15. Double Scan ROC Curve for a PMA-1A AT Mines at 5-6 cm Taken on the Morning of October 28.

In real time in the field, it was difficult to assess exactly how well the system was performing. It was possible that in going from the single scan sequence for the AT mines to the double scan used for the AP mines, some of the settings in the pulse sequence were not set to their optimum values or that the system software contained an error when taking or combining the results of a double scan. Therefore, on October 29 the tests were temporarily halted and effort focused on determining the performance on AP mines. After a number of unreliable measurements, the ROC curve shown in Figure 16 was taken with carefully checked pulse sequence and data analysis parameters.

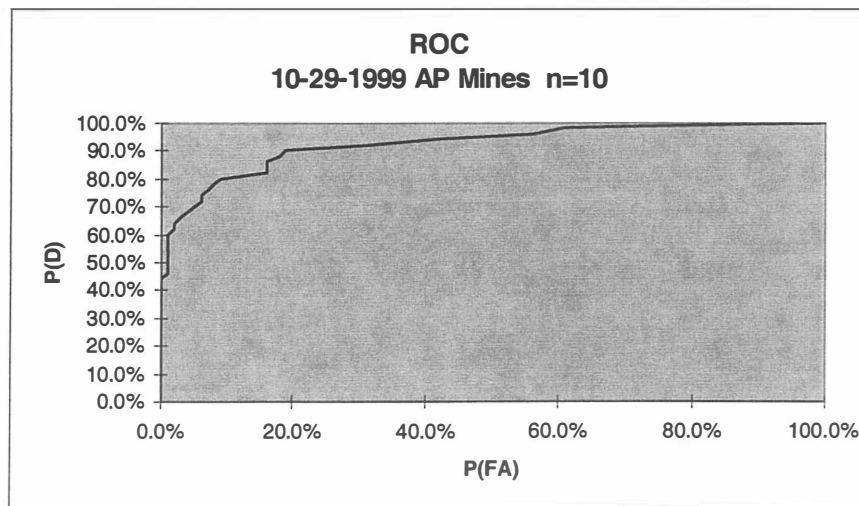


Figure 16. ROC on a PMA-1A Mine at 6 cm. Ten Scans per Data Point- October 29.

This curve should be compared to the PMA-1A data shown in Figure 17 for a mine at a higher temperature and taken in a shielded room. At this point, it became clear that some form of component failure caused the system operation on the second half of the test to be degraded by

about a factor of about four in terms of system sensitivity. After a day of system debugging on Saturday, October 30, it was decided to halt the test and return the system to San Diego for repair.

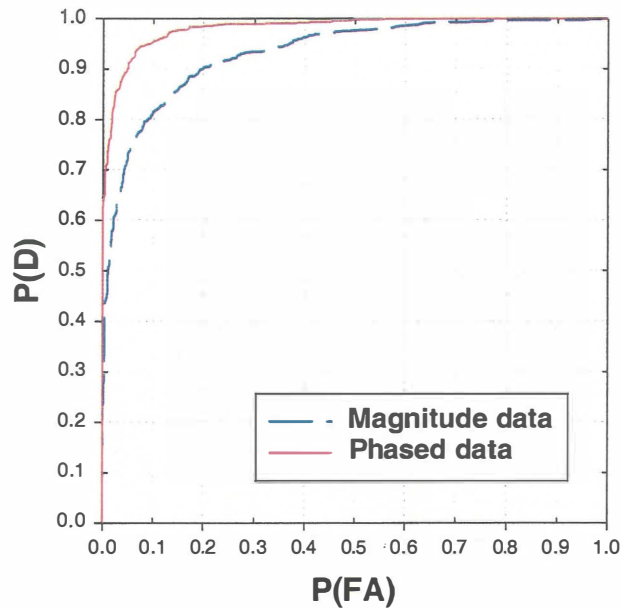


Figure 17. ROC Curve on a PMA-1A Mine Taken in San Diego. Mine temperature is 21°C. Phase data (red) corresponds to the processing used at Ft. Leonard Wood in October 1999.

Despite these problems, the NQR system was able to identify all 23 AT targets; the detection threshold could be set to give 100% probability of detection (PD). Strictly speaking, the probability of false alarm (PFA) depends on the definition of the region around the mine (the halo) which counts as a true detection. However, it is clear from Figure 14 that the overall number of false alarms is less than 5. Given that there were approximately 1000 measurements taken in Figure 14, the $PFA < 0.5\%$. For the test on the first day (upper data in Figure 14), the detection threshold could be set to give $PD = 100\%$, $PFA = 0\%$. The RFI level during the last hour of both days of AT tests was 1000 times higher in power than the NQR signal.

The sensitivity profile of the detection coil used in these tests is such that it has moderate sensitivity for a mine up to about 15 cm from its center. A mine with a very large mass, such as a shallow AT mine, will produce a clearly detectable signal at such range. The NQR and metal detection signal are plotted as a function of distance to the nearest mine in Figure 18.[4] The localizing capability of the coil is clearly evident. Given that the mines are approximately 30 cm across, it is evident that the small NQR detection coil used at Ft. Leonard Wood can localize them to within a few centimeters of their outer edges.

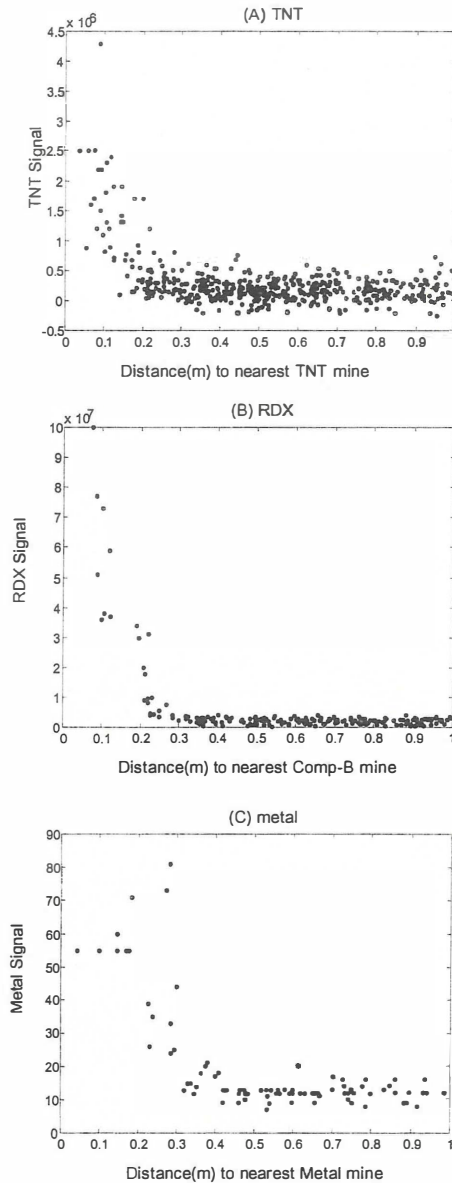


Figure 18. (A) TNT, (B) RDX, and (C) Metal Signal Measured versus Miss Distance to the nearest Mine (figure courtesy Reference 4).

4.2.3 Antipersonnel Mine Detection Test

Owing to their smaller mass, detection of buried AP mines is a more demanding test of the system. The QR prototype was repaired and debugged in San Diego and returned to Ft. Leonard Wood on November 29, 1999. An AP test lane similar to the AT test lane was set up to provide a comparable test. The lane was 4.48 m x 1.12 m and contained seven PMA-1A mines and five VS50 mines. The mine characteristics are summarized in Table 5.

Table 5. A Summary of the AP Mines Used in the Test. The quantities d, h, l, and w stand for diameter, height, length, and width.

AP Model	Case Material	Main Charge	Size (cm)	Country of Origin
PMA-1A	plastic	200 g TNT	l=14, w=7, h=3	former Yugoslavia
VS-50	plastic	43 G RDX	d=9, h=4.5	Italy

A total of three separate passes of the lane were carried out on the same day. A single scan 0.58 seconds long was used for each cell. The results for the TNT mines are plotted in Figure 19a using the threshold set prior to the test. This threshold was based on historical measurements and was not optimized for the test site or for weather conditions. Each pass of the mine lane required 256 discrete measurements. Each mine was detected in all three passes of the lane (i.e. PD = 100%). For the initial threshold, the number of false alarms for each pass was 22, 7, and 14.

By comparing successive passes, it is possible to determine the effect of rescanning all the initial alarms. The results are shown in Figure 19b. If the alarms in Pass 1 are confirmed by the results of the result of the subsequent measurement of the same cell in Pass 2, then all of the true detections remain but all of the false alarms are removed. The same complete clearance is achieved by comparing Pass 3 with the initial alarms of Pass 2. Combining Pass 3 and Pass 1 produces two remaining false alarms corresponding to 0.4 per m².

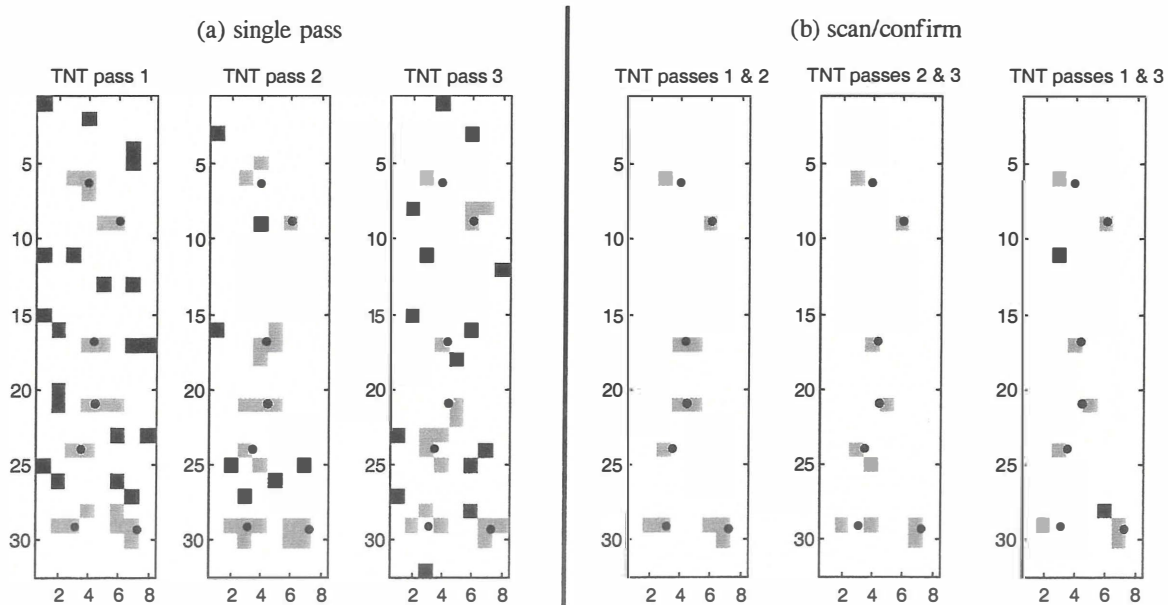


Figure 19. Results of Single Passes (a) and Scan/Confirm Scheme (b) on 7 PMA-1A TNT-filled AP Mines. Grey clusters are detections and black clusters are false alarms. Black dots mark the locations of the mines. The TNT threshold used was chosen at the test. A single scan of 0.58 seconds was used for each cell. Data taken from reference 4.

The combined signal for all three passes for TNT, RDX and metal is shown in Figure 20. The location of all 7 TNT AP mines is clearly visible. Markers placed on the plastic sheet during the test were later all found to lie with in the area of the individual mine cases. The system was also able to detect all five VS50 RDX mines. However, given the system problems and the greater importance of TNT detection in this test, the RDX detection parameters were not changed from their previously unoptimized values used for the tests on October. It should be noted that the VS50s also gave a clear metal signal which is thought to be due to a metal locator plate within them.

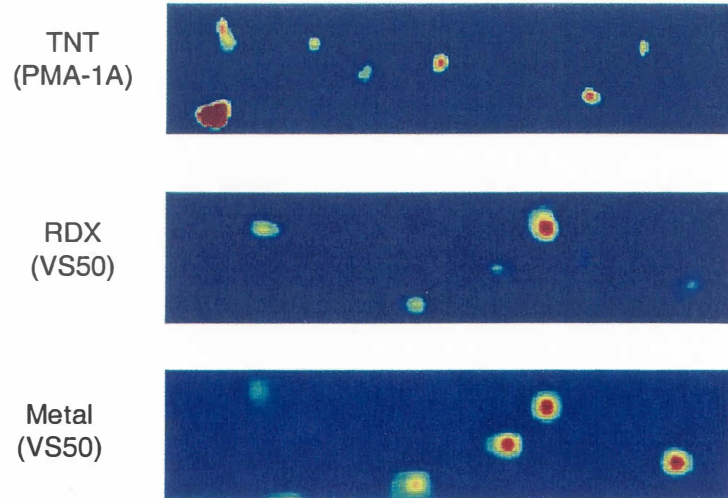


Figure 20. Image of Output SNR for AP Mine Test. Sum of all three runs made on December 1.

To get an accurate assessment of the system SNR, a 100-point ROC curve was taken on a PMA-1A mine on the day after the AP lane test using a single TNT scan of 0.58 s. The surface temperature of this mine was measured to be 7°C. The result, shown in Figure 21, should be compared to ROC on exactly the same mine that was taken on October 29. The December result clearly indicates that the system was operating at significantly reduced sensitivity in the second half of the AT lane test on October 28 and possibly before that also.

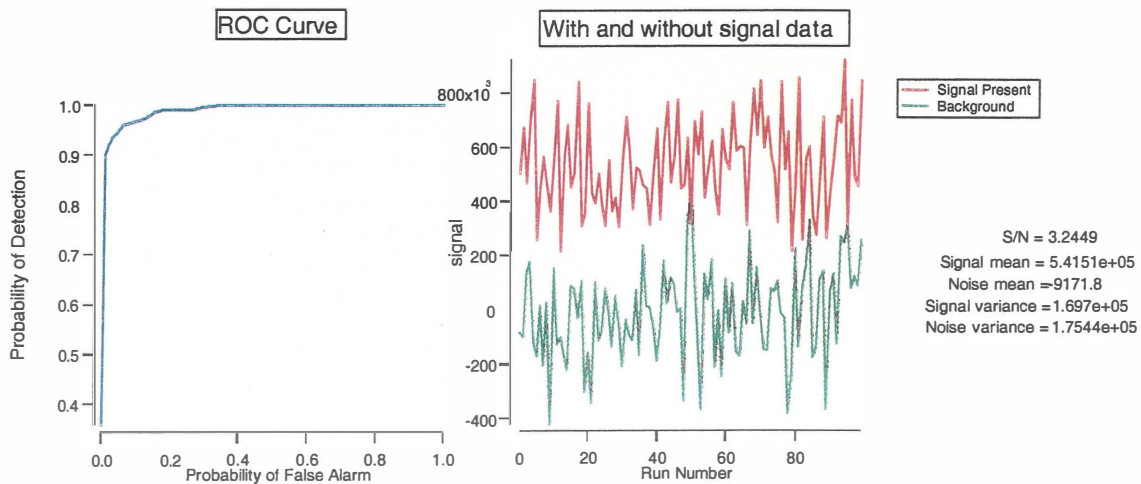


Figure 21. In Field ROC Curve on PMA-1A Mine at 7°C.

4.2.4 Summary of Test Results

A series of field tests under blind conditions was carried out on a first prototype NQR landmine detection system. The test results, summarized in Table 6, show that extremely high PD and very low PFA can be achieved on mines or on surrogate mines with zero metallic content. These results are particularly important because they show that contrary to prior expectations, TNT can be clearly detected by NQR. It should also be noted that, to date, NQR has not missed a single mine in any of the blind tests.

Table 6. Summary of Test Results under Blind Conditions on Prototype NQR Landmine Detection System.

Test	PD	PFA	Notes
Eagle Base Bosnia, AP	100 % (7 out of 7 RDX, 1 out of 1 metal)	0%	Initial PFA < 5%, resolved by 2 out of 3 voting
Ft. Leonard Wood, AT	100% (20 of 20 TNT, 2 of 2 Composition B, 1 of 1 metal)	< 0.5%	No rescanning, alarms due to system component failure.
Ft. Leonard Wood, AP	100% (7 of 7 TNT, 5 of 5 RDX/metal, all three passes)	< 1%	Rescanning initial alarms gave 0, 0 and 0.4 false alarms per m ² .

5. CONCLUSIONS AND RECOMMENDATIONS

This program has been a major technical success, showing for the first time that landmines buried in typical field conditions can be detected by their chemical signature. The system has demonstrated detection performance equal to, or better than, any other advanced technology, including those that have been under development for many years. Furthermore, major strides have been made in the understanding of QR and how to construct QR systems. Much of this understanding has only partly been incorporated in the prototypes described in this report. The success to date and the new knowledge bodes well for the further improvement of QR for landmine detection and its eventual contribution to removing the landmine threat.

It is important to note that this program has provided a truly new measurement modality for the landmine detection problem. The QR result is orthogonal to the presently used methods of metal detection and ground penetrating radar, and therefore provides an ideal additional measurement channel, that can be used simultaneously to provide a joint detection decision with another sensor, or afterwards in an alarm resolution mode. The value of the additional information from QR and its flexibility in use should not be underestimated for a problem as intractable as landmine detection. Indeed, given the wide variety of environmental conditions, mine types and mission tempos, it is likely that no fixed combinations of sensors will be satisfactory, but that different sensors will be emphasized depending on the requirements in the field.

Towards this end, the Army and Navy have initiated separate programs to further QR technology for specific mine detection missions. Under a 30-month Army program, large QR coils are being developed for vehicle mounted road clearance applications. Two specific measurement scenarios are required: a) stationary operation of a very large QR coil to resolve regions indicated by a combined GPR and metal detection measurement from a primary road clearance system, b) a moving array of QR coils sufficient to scan the entire width of a road while in motion. Under the Navy program, QR is being extended to detect smaller AP mines and mines containing the explosive tetryl. In addition, the QR hardware is being reduced in size and weight so that the entire system can be carried by a single user.

Given the continuing R&D investment and the rapid progress to date, it seems likely that this DARPA program will have provided a significant contribution towards addressing the landmine threat.

This document reports research undertaken at the U.S. Army Soldier and Biological Chemical Command, Soldier Systems Center, and has been assigned No. NA/TICK/TR-011007 in a series of reports approved for publication.

REFERENCES

1. Hibbs, A.D., Barrall, G.A., Beevor, S., Burnett, L.J., Derby, K., Drew, A.J., Gregory, D., Hawkins, C.S., Huo, S., Karunaratne, A., Lathrop, D.K., Lee, Y.K., Matthews, R., Milberger, S., Oehmen, B., Petrov, T., Skvoretz, D C., Vierkötter, S.A., Walsh, D.O., and Wu, C. Field Test Results of a Nuclear Quadrupole Resonance Landmine Detection System. Proc. SPIE 4038 (Detection and Remediation Technologies for Mines and Minelike Targets V), in press.
2. Hibbs, A.D., Barrall, G.A., Czipott, P.V., Drew, A.J., Gregory, D., Lathrop, D.K., Lee, Y.K., Magnuson, E.E., Matthews, R., Skvoretz, D.C., Vierkötter, S.A. and Walsh, D.O. Detection of TNT and RDX Landmines by Stand-off Nuclear Quadrupole Resonance. Proc. SPIE 3710 (Detection and Remediation Technologies for Mines and Minelike Targets IV), pp. 454-463, 1999.
3. Hibbs, A.D., Barrall, G.A., Czipott, P.V., Lathrop, D.K., Lee, Y.K., Magnuson, E.E., Matthews, R. and Vierkötter, S.A. Landmine Detection by Nuclear Quadrupole Resonance. Proc. SPIE 3392 (Detection and Remediation Technologies for Mines and Minelike Targets III), 522-532, 1998.
4. Rotondo, F. and Ayers, E. Antitank and Antipersonnel Mine Detection Results for a Nuclear Quadrupole Resonance Landmine Detection System. IDA Document D-2444, in preparation.